Protein Ultrafiltration: A General Example of Boundary Layer Filtration

A rotating disk membrane was developed to investigate experimentally concentration polarization during the ultrafiltration of bovine serum albumin solutions. The experimental data supported analytical and numerical predictions which were developed as part of this study. Osmotic pressure and concentration dependent viscosity and diffusivity were demonstrated to be important factors. The results were also extended to predict ultrafiltration in porous walled ducts. Finally, a formal description of protein ultrafiltration in terms of the Stephan-Maxwell flux equations was shown to provide a unifying description of all filtration processes from mechanical filtration to reverse osmosis.

A. A. KOZINSKI and E. N. LIGHTFOOT
Department of Chemical Engineering
University of Wisconsin
Madison, Wisconsin 53706

SCOPE

One of the current intensively investigated methods for concentration and purification of materials is that of membrane separations. It has been applied to separations which are difficult by other methods because membrane systems offer mild operating conditions, simplicity, potentially high selectivity and, for some cases, low energy requirements. These make membrane separations particularly attractive for biological materials which are generally very sensitive to their environment. However, severe performance limitations are encountered due to the buildup of concentrated boundary layers of rejected macrosolutes on the membrane surface. This problem, called "concentration polarization," while not unique to protein ultrafiltration is particularly severe with proteins since they tend to sludge or gel in concentrated solutions. This gel can effectively stop flow through the ultrafiltration membrane by creating a large hydrodynamic resistance in addition to the usual thermodynamic resistance. A need exists for predicting the occurrence of this protein sludge layer and if possible to find ways to reduce or control the effects.

The boundary layer analytical models developed in the literature for ultrafiltration specifically do not account for the highly concentration dependent viscosity and diffusivity of protein solutions, and more basically these models suffer from adequate experimental verification. Several previous experimental studies of protein ultrafiltration have been conducted but generally only in flow situations too complex for unambiguous analysis. For reliable analysis one must be able to separate behavior peculiar to the configuration—so called boundary layer effects—from membrane characteristics. To determine the utility of any given diffusional model of ultrafiltration one must be able to provide a complete a priori description which can be tested unambiguously by experiment. The rotating disk provides such a simple well-defined system with which to analyze this very complex behavior. Such a study has not previously been made.

The simple models developed for the well-defined situation can then be extended to the more practical but also more complicated tube and parallel plate configurations. Finally, it is useful to recognize that ultrafiltration has the essential characteristics of both mechanical filtration and reverse osmosis. A satisfactory analysis of this process thus provides a unified description of nonisobaric boundary layer filtration processes.

CONCLUSIONS AND SIGNIFICANCE

The results of this study, while not specifically demonstrating how concentration polarization can be reduced, do present an improved interpretation of ultrafiltration and do point out what are the real problems in controlling protein ultrafiltration.

The basic similarity between all filtration processes from reverse osmosis to hydrodynamic filtration is exemplified by protein ultrafiltration which encompasses both thermodynamic and hydrodynamic filtration. A formal description in terms of the Stephan-Maxwell flux equation was developed which is valid for all boundary layer filtration processes. Although difficult to employ at present because of limited data, the description is a useful unifying view and represents an area for future study.

It was shown that concentration polarization effects for a well-defined protein system could be analyzed by relatively simple boundary layer techniques. A permeable rotating disk in a confined solution was demonstrated to be

° A. A. Kozinski is with the Department of Chemical Engineering, University of Illinois, Urbana 61801.

an excellent tool for unambiguous experimental evaluation of boundary layer effects in ultrafiltration as predicted by analysis.

Osmotic pressure and concentration dependent viscosity and diffusivity were shown to be important factors in the ultrafiltration models developed for rotating disk flow. However, average physical property values were found to be adequate in many situations. By recognizing the simplifications possible for the high Schmidt numbers of protein solutions, the predictions of the effects of concentration polarization were extended to tube and parallel plate geometries. Based on available data from the literature, this approach yielded surprisingly accurate predictions. The form for all of these correlations was that of the standard Nusselt number for mass transfer but with correction factors for property variations. In ultrafiltration the Nusselt number is directly proportional to the permeation velocity through the membrane.

In general these predictions represent an ideal limit to actual performance. This limit is imposed by the physics of the process and is in fact difficult to remove. However, of practical importance is the avoidance of conditions which lower performance well below this limit. The severe drop in permeation rate caused by sludging and gelling was not predictable by simple diffusion models. The chemistry of the protein solution was the critical factor in sludge formation. The dependency of sludge formation on pH, ionic strength, incompatible solutes, and other conditions is the critical information which is not available for predicting actual performance. Future emphasis in ultrafiltration is needed on the chemical solution properties which have great potential for improved operations.

DESCRIPTION OF BOUNDARY LAYER PROBLEM

In ultrafiltration as in all convective mass transfer processes, a fundamental quantitative description is obtained by solution of the equations of motion, species continuity, equations of state, and species flux expressions for a particular set of boundary conditions. The particular factors which distinguish ultrafiltration from ordinary convective transfer are (1) a non-negligible velocity through the membrane boundary of the system (2) unusually large concentration polarization resulting from solute rejection and the low diffusivity of proteins.

In principle, many studies on boundary layer mass transfer (Acrivos, 1960b; Stewart, 1963) with finite wall velocities and the abundant studies on reverse osmosis can be applied to ultrafiltration. In practice, however, the ranges of permeation rates and physical properties are so different that these papers are of limited value. In particular, the large effects of protein concentration on physical properties, viscosity and diffusivity, and thermodynamic properties, osmotic pressure, and solubility must be specifically considered.

A convenient starting point is the description of the rate equations which relate mass fluxes to driving potentials in this concentration polarized boundary layer. The generalized multi-component equations as formulated by Scattergood and Lightfoot (1968) are applied as follows,

$$d_i = \sum_{\substack{j=1 \\ \neq i}}^{m} \frac{X_i X_j}{\mathcal{D}_{ij}} (V_j - V_i) = \sum_{\substack{j=1 \\ \neq i}}^{m} \frac{1}{C_m \mathcal{D}_{ij}} (X_i N_j - X_j N_i) \quad (1)$$

$$d_i = \frac{X_i}{RT} \nabla_{TP} \tilde{\mu}_i + \left(X_i \bar{V}_i - \frac{\tilde{\omega}_i}{C_m RT} \right) \nabla P - \frac{\rho_i}{C_m RT} \left[g_i - \sum_{k=1}^{m} \tilde{\omega}_k g_k \right] \quad (2)$$

with $\Sigma d_j = 0$, $\mathcal{D}_{ij} = \mathcal{D}_{ji}$. The number of species is usually quite large. However, in ultrafiltration all small solutes move with the water while protein is rejected. The small solutes, except for a small number of counter-ions which stay with the protein, then may be included with water as a total solvent s. Thus, the system may be treated as pseudo binary, and Equation (1) becomes

$$d_p = \sum_{\substack{j=1 \\ \neq p}}^{m} \frac{X_p X_j}{\mathcal{D}_{pj}} (V_s - V_p) = \frac{X_p X_s}{\mathcal{D}_{ps}} (V_s - V_p) \quad (3)$$

$$\frac{X_s}{\mathcal{D}_{ps}} = \sum \frac{X_j}{\mathcal{D}_{pj}} \quad (4)$$

This then defines a binary coefficient for the diffusion of protein through solvent as in the usual form of Fick's Law. The presence of a large number of small neutral solutes, indifferent electrolytes, also allows any electrodiffusion effects to be neglected.

It remains now to explicitly define the body forces in Equation (2). This is simplified by the usual boundary layer approximations, namely,

1. Diffusion takes place perpendicular to the phase boundary (membrane).
2. Mechanical equilibrium exists across the boundary layer.

For these conditions, the body forces may be written as

$$(g_s)_y = g_y \quad (5)$$

$$(g_p)_y = g_y + \frac{1}{\rho} \frac{\partial P}{\partial y} \quad (6)$$

where y is the direction perpendicular to the membrane and g is the gravitational acceleration. Equation (6) follows from the arguments of Scattergood and Lightfoot (1968) regarding a species immobilized by a mechanical support and in mechanical equilibrium across the boundary layer. The rejected proteins transmit an equivalent body force from the supported membrane. The flux of solvent across the boundary then becomes

$$N_{sy} - X_s (N_{py} - N_{sy}) = - \frac{C_m \mathcal{D}_{ps}}{RT} \left[X_s \frac{\partial}{\partial y} \tilde{\mu}_s + X_s \bar{V}_s \frac{\partial P}{\partial y} \right] \quad (7)$$

$$= - C_m \mathcal{D}_{ps} \left[\left(1 + \frac{\partial \ln \gamma_s}{\partial \ln X_s} \right) \frac{\partial X_s}{\partial y} + X_s \frac{\overline{V}}{RT} \frac{\partial P}{\partial y} \right]$$

In the other directions the species velocities are $V_s \cong V_p$ for the approximations of this study.

This simple result presents the opportunity to treat the previously unrelated processes of reverse osmosis and mechanical filtration from a unified point of view. The ultrafiltration of materials, like proteins, represents a situation intermediate between the purely diffusional behavior encountered in reverse osmosis and the purely hydrodynamic nature of ordinary filtration. This can be applied as follows:

1. In reverse osmosis, the boundary layer is treated as an ideal dilute solution for which the pressure gradient will be zero. Equation (7) then simplifies to the familiar form of Fick's Law for a binary solution.

2. In mechanical filtration, the solute is deposited or precipitates at the boundary. These restrained solutes can now transmit an equivalent body force from the supported membrane. In addition, the gradient in chemical potential approaches zero as the solute becomes totally immobilized. The coefficient of the pressure gradient is now the hydrodynamic resistance of this sludge layer and can be obtained from conventional expressions for flow through porous media.

3. In ultrafiltration, both effects can be important since proteins in solution behave both as hydrodynamic particles of finite size and as part of the continuum. At low levels of polarization, chemical potentials predominate as in reverse osmosis. At high levels of polarization the protein precipitates or gels and hydrodynamic potentials predominate as in ordinary filtration.

The most interesting condition is that of highly concentrated solutions which have not gelled. The protein molecules may still to a degree transmit a body force from the membrane, but the chemical potential gradient is not zero. In general, one will not be able to distinguish between the effect of chemical potential gradient and pressure gradient without an intimate knowledge of the molecular properties of the solution. The usual approach is to lump the pressure and chemical potential into one term.

$$\tilde{u}_{\text{tot}} = \tilde{u}_s + P \overline{V}_s \tag{8}$$

This total potential is then expressed in terms of a new activity coefficient. The resulting diffusion coefficient D'_{ps}, when measured in dilute solutions where the pressure gradient is zero, is identical to Equation (3). However, as pointed out above, in concentrated solutions the pressure gradient cannot be neglected and D'_{ps} no longer correctly represents the diffusion behavior.

At present, insufficient thermodynamic data are available to employ Equation (7) correctly to evaluate the concentrated boundary layers which occur in ultrafiltration. However, the single expression is still an appropriate description of all boundary layer membrane processes and can be used as an aid in interpreting observed performance.

ULTRAFILTRATION IN A WELL-DEFINED SYSTEM

The application of this description to the analysis of real ultrafiltration systems requires the simultaneous solution of the diffusion equation and the equations of motion. These equations are coupled through highly concentration-dependent physical properties. We will initially consider here the case of Newtonian flow about a rotating disk which results in a considerably simplified analysis since the defining equations both for mass and momentum transfer may be expressed in terms of a single independent variable. The well-known high Schmidt and Reynolds number boundary layer simplifications are applicable to protein ultrafiltration and reduce the analysis to an even simpler form. The equation of motion is approximated by assuming the shear stress is constant within this concentrated layer. The description of protein ultrafiltration then takes the following form:

$$C_m V_Z \frac{dX_p}{dZ} = \frac{d}{dZ} C_m D_{ps} \frac{dX_p}{dZ} \tag{9}$$

$$\tau_{RZ} = - \mu_p \frac{dV_r}{dZ} \tag{10}$$

The value of τ_{RZ} is determined by matching with the constant-property shear stress outside the concentration boundary layer. The boundary conditions for ultrafiltration are

$$Z = 0 \qquad V_r = 0 \tag{11a}$$

$$X_p V_Z|_W = D_{ps} \frac{dX_p}{dZ}\bigg|_W \tag{11b}$$

$$V_Z = - K(\Delta P - \pi) \tag{11c}$$

$$Z = \infty \qquad X_p = X_b \tag{11d}$$

Note that osmotic pressure π is a function of protein concentration at the membrane.

The problem can be made dimensionless by using the usual transformations and by recognizing the calculations of Olander (1962) which showed that variable density effects in the continuity equation are an order of magnitude less than the effect of variable density in the diffusion equation. We, thus, obtain

$$\rho \, Sc \, H \frac{d\theta}{d\eta} = \frac{d}{d\eta} \rho \, D \frac{d\theta}{d\eta} \tag{12a}$$

$$\tau_0 = 2F'\mu \tag{12b}$$

$\eta = 0$

$$H = - K(\Delta P - \pi(\theta)) \tag{13a}$$

$$\frac{d\theta}{d\eta} = \frac{Sc \, H}{D} (\theta + 1) \tag{13b}$$

$$F = 0 \tag{13c}$$

$\eta = \infty$

$$\theta = 0 \tag{13d}$$

where

$$\eta = Z \left(\frac{\omega}{\nu_b} \right) \tag{14a}$$

$$H(\eta) = V_Z/(\nu_b \omega)^{1/2} \tag{14b}$$

$$F(\eta) = V_r/(r\omega) \tag{14c}$$

$$\theta = (X_p - X_{pb})/X_{pb} \tag{14d}$$

Two important factors appear in our analysis which are required for a description of ultrafiltration; namely, variable physical properties which provide a way to account for gelling and the osmotic pressure which is included through boundary condition (13a).

TABLE 1. NUSSELT NUMBERS FOR ROTATING DISK ULTRAFILTRATION

$$Nu = A\,Re^{1/2}\,Sc^{1/3}$$

a. Numerical calculation, variable properties as in Equation (15).

$$A \equiv 0.9\left(\frac{X_{pW}}{X_{pb}}\right)^{1/3}$$

b. Asymptotic approximation, constant properties

$$A = 0.98\left(\frac{X_{pW}}{X_{pb}}\right)^{1/3}$$

c. Asymptotic approximation, variable properties linearly approximated at boundary.

$$A \simeq \left(\frac{\tau_0 X_W^*}{X_b^*}\right)^{1/3}\left(\frac{D_W^2}{\mu_W}\right)^{1/3}(\text{correction terms})^{1/3}$$

$$\text{correction terms} = \frac{\left(1 + \frac{\mu_W}{\mu_{corr}} + 8\frac{\rho_W}{\rho_{corr}} + 5\frac{D_W}{D_{corr}}\cdots\right)}{\left(1 + \frac{\rho_{corr}\,C_W^*}{\rho_W\,C_b^*} + \frac{2\rho_{corr}\,D_W\,C_W^{*2}}{\rho_W\,D_{corr}\,C_b^{*2}}\cdots\right)}$$

EQUATIONS OF STATE

As indicated earlier, a knowledge of the thermodynamic and transport properties of concentrated protein solutions is essential to the analysis of ultrafiltration since π, μ, and D all show large changes with concentration. In general, this type of data is not available. However, bovine serum albumin solutions are an exception and for this reason were chosen for the experimental work of this study. The specific data for bovine serum albumin solutions are described briefly in Appendix B and at more length by Kozinski (1971).

More generally, based on scanty evidence, globular protein solutions appear to be nearly Newtonian and the viscosity coefficient μ can be described by the following empirical modification of the Einstein relation:

$$\frac{\mu}{\mu_0} = \frac{1}{1 - 2.5\,\tilde{\alpha}\,\Phi} \tag{15}$$

Here $\tilde{\alpha}$ is an empirical constant characteristic of the protein. Additional improvements have been suggested based on data for concentrated suspensions and colloidal sols by Ford (1960). These corrections take the form of higher order concentration terms in the denominator of the above expression.

There is considerably more uncertainty as to the diffusion behavior of concentrated protein solutions. The available data are those of Keller et al. (1971) who found very similar concentration dependences for hemoglobin solutions and bovine serum albumin solutions. Diffusion data are quite difficult to obtain and may be the greatest source of uncertainty in the prediction of ultrafiltration performance.

ANALYSIS OF ULTRAFILTRATION

The numerical integration of these equations has previously been described by Kozinski and Lightfoot (1971) for the limiting case of protein sludging or gelling before a significant osmotic pressure is developed. The more general case can be obtained by formally integrating Equations (12) to (15).

$$\frac{\theta_W}{1+\theta_W} = Sc\,H_W\,\rho_W\int_0^\infty\left(\frac{1}{\rho D}\exp\int_0^\eta\frac{Sc\,H}{D}\,d\eta'\right)d\eta'' \tag{16}$$

Following the work of Acrivos (1960a), we would expect a solution of the following form for rotating disk mass transfer where the permeation rate which is related to pressure drop is expressed as a Nusselt number.

$$Nu_{LOC} = A\,Re^{1/2}\,Sc^{1/3}\ ^{*} \tag{17}$$

The coefficient A will reflect the particular physical property variations and conditions of the system. Values of A for several different models are shown in Table 1. The first entry is from our previous numerical solutions which neglected osmotic pressure and expressed the condition of gelling as an infinite viscosity coefficient at the membrane surface.

Equation (16) can also be integrated using standard asymptotic expansions for the exponential arguments. Entry *b* in Table 1 is the result for constant physical properties which agrees quite well with the previous numerical result. The integration for variable physical properties can also be performed using asymptotic expansions. The actual physical property functions can be approximated with an assumed linear concentration profile near the boundary. These linear approximations provide considerable mathematical convenience and at the same time acceptable accuracy since errors in the description of μ and D in the intermediate region of the boundary layer are of secondary importance. With the following linear concentration profile,

$$\theta = \theta_W + \left.\frac{d\theta}{d\eta}\right|_W \eta \tag{18}$$

$$= \theta_W + \frac{Sc\,H_W}{D_W}(1+\theta_W)\eta$$

the variable property functions can be expressed as follows:

$$\rho = \rho_W + \rho_{corr}\left.\frac{d\theta}{d\eta}\right|_W \eta \tag{19a}$$

$$\frac{1}{D} = \frac{1}{D_W} + \frac{1}{D_{corr}}\left.\frac{d\theta}{d\eta}\right|_W \eta \tag{19b}$$

$$\frac{1}{\mu} = \frac{1}{\mu_W} + \frac{1}{\mu_{corr}}\left.\frac{d\theta}{d\eta}\right|_W \eta \tag{19c}$$

With these simplifications the exponential argument in Equation (16) becomes a power series in η. Using the asymptotic expansions the results shown in Table 1 can be obtained.

The form of the solution is similar to that expected from a perturbation analysis. Higher order approximations confirm this interpretation in that only the correction term is changed by improved concentration profiles.

The important result of the variable property analysis is the form of the major variable-property factor D_W^2/μ_W. The density appears only in the second-order correction terms and even here only to a secondary degree. Except in situations where natural convection can occur, its varia-

* The definition of the Nu_{LOC} follows from the usual definition Bird et al. (1960) used with Equation (14*c*). This results in $Nu_{LOC} \equiv (-V_{y0}\,d/D_{pW})\,(X_{p0}/X_{p0} - X_{p\infty})$.

tion can be neglected compared to that of viscosity and diffusivity variations. The variable property factor D_W^2/μ_W is an extreme correction based on using the membrane, where the protein concentration is at its maximum value, as the origin for the expansions. The second-order correction terms must be used if a reasonable result is to be obtained. However, the scarcity of viscosity and diffusivity data in the critical high concentration range makes effective application of this procedure difficult at present. This is clearly a subject for further study.

EXPERIMENTAL STUDIES WITH BOVINE SERUM ALBUMIN

Experimental studies of rotating disk ultrafiltration were performed with serum albumin solutions. The results of these studies which are discussed below, compare quite well with the predictions of the developed models for situations in which the protein has not denatured.

Experimental Results

The experimental work was performed with crystallized fraction V, bovine serum albumin solutions with the purity checked regularly (Kozinski, 1971). The available physical property data for these solutions are discussed in Appendix B along with new viscosity data obtained as part of this study. The experimental disk system specifically designed and constructed for this study is shown in Figures 1 and 2. Details of this design are available elsewhere (Kozinski, 1971). A summary of the experimental data obtained with this unit are shown in Figure 3; each data point represents an average of several observations.

Qualitatively the curves in Figure 3 conform to our postulated concentration diffusion models. At low permeation velocities, corresponding to low levels of concentration polarization, the protein curves coincide with the pure buffer line since osmotic pressure is truly negligible at low concentrations of protein. As the pressure is increased and the permeation level rises, the surface concentration reaches the point where significant osmotic pressures are developed. The curves now begin to deviate from the pure buffer curve. The pressures at which the curves deviate from the pure buffer line are determined by the Schmidt and Reynolds numbers.

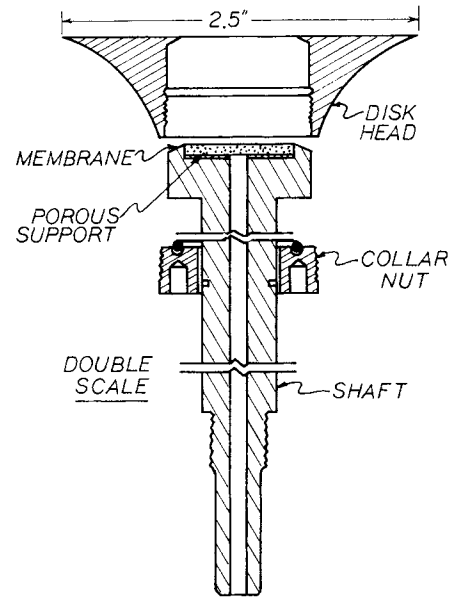

Fig. 2. Rotating disk.

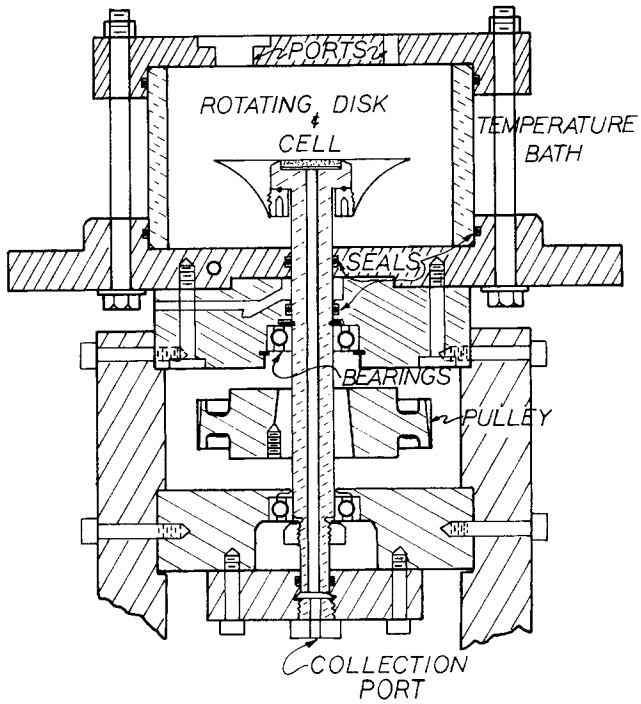

Fig. 1. Equipment section.

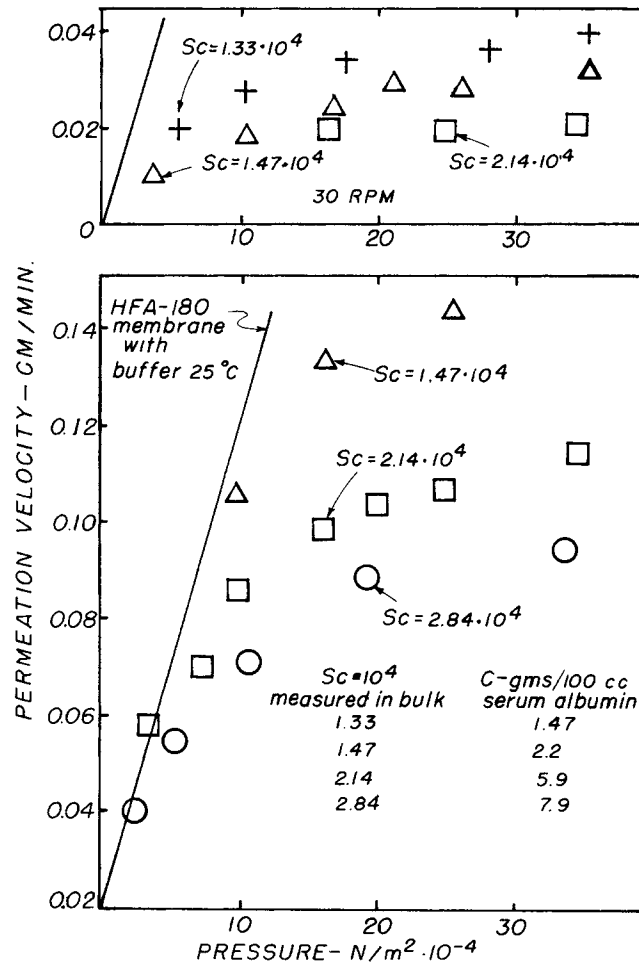

Fig. 3a. Protein permeation rates.

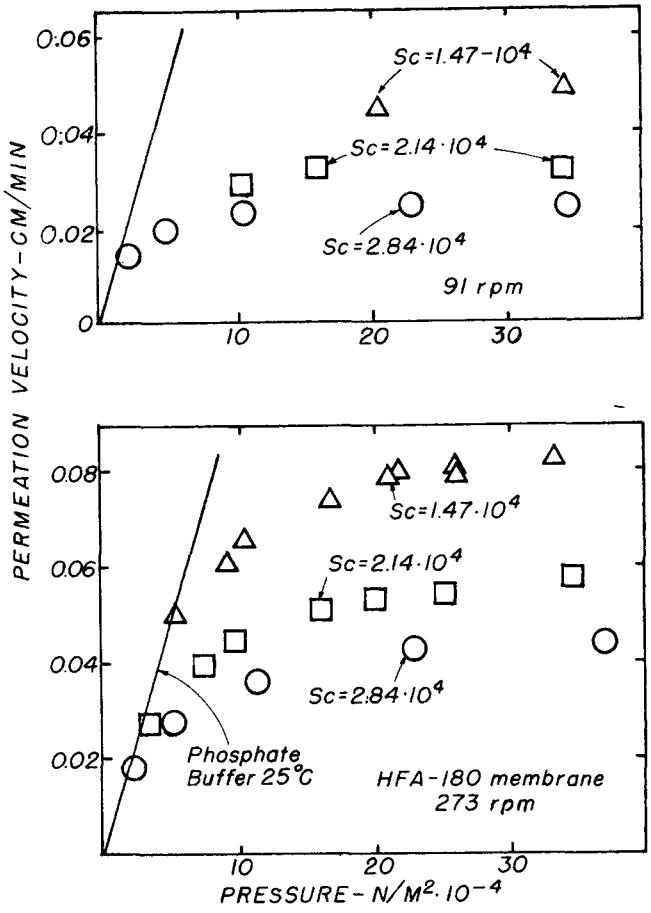

Fig. 3b. Protein permeation rates.

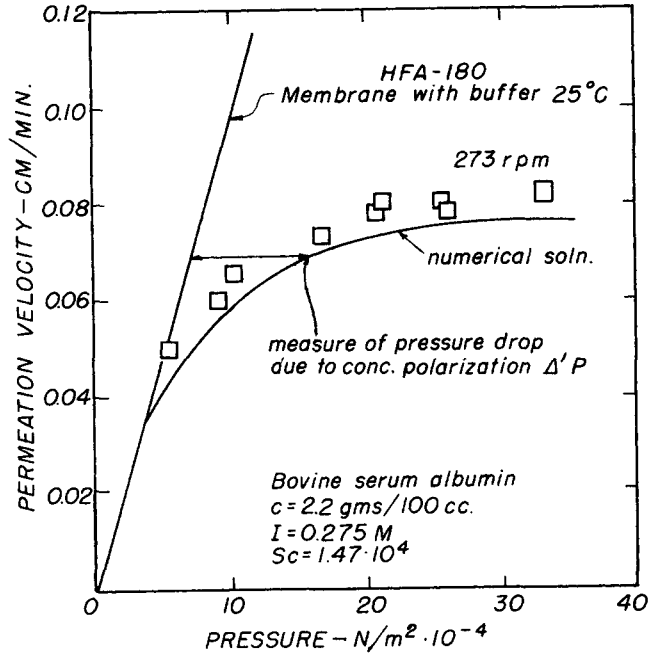

Fig. 4. Model prediction.

At any given permeation velocity, the pressure difference between the pure buffer line and the protein solution curve can be interpreted as a measure of the osmotic pressure. One can take the alternate view that this deviation represents a significant hydrodynamic resistance in the boundary layer. However, for serum albumin we feel the evidence indicates that the osmotic pressure is by far the dominant contribution. First, serum albumin is an extremely soluble rigid protein molecule. The osmotic pressures measured from these curves correspond to surface concentrations well below the solubility limit. Thus, a hydrodynamic resistance due to precipitation is not likely. The protein has not crosslinked in solution because the data points are totally reproducible even after total polarization. That is, no hysteresis was found when operations were varied between totally polarized and partially polarized conditions. This indicates that the proteins are still mobile in solution. Also the concentrated boundary layers are very thin and any pressure drop due to hydrodynamic drag is quite small. Finally, the osmotic pressure of serum albumin does apparently become extremely large at high protein concentrations and would necessarily represent a considerable portion of any deviation.

The data were taken up to a pressure of only $34.5 \cdot 10^4$ N/m² because of the structural limitation of the HFA-180 membrane (Abcor Inc.) used throughout this study.

Comparison of Prediction and Experiment

The osmotic interpretation of the data is substantiated by a numerical solution of the osmotic diffusion model for the specific conditions of the experiment. The physical property data for serum albumin solutions which are discussed in Appendix B were used in the diffusion model represented by Equations (12) to (14).

A result of this solution which was by a standard 4th order Runge Kutta method is shown in Figure 4 for one set of experimental conditions: 273 rev./min. and c = 2.2 g./100 cc. The agreement with the experimental data is excellent and is well within the accuracy of the physical property data. This was also true for the other experimental conditions. The numerical solution was very sensitive to the exact behavior of the diffusivity, osmotic pressure, and viscosity at high concentrations. This numerical approach would, therefore, not be very useful with less completely characterized proteins. However, the solution does agree with the osmotic-diffusion model interpretation of ultrafiltration for serum albumin.

The experimental data can also be used to evaluate the analytical approximations discussed earlier. To do this, we first note that the boundary layer approximation requires that

$$Nu \propto Re^{1/2}$$

or that

$$V \propto Re^{1/2} \tag{20}$$

(Re is evaluated at bulk conditions) for constant interfacial conditions. Good agreement between this prediction and the data is shown in Figure 5 for the totally polarized interfacial condition. Agreement at the other conditions was equally good.

One can now check physical property effects of the analytical approximation, Equation C, Table 1. To facilitate comparison between predicted and observed, the following quantities are defined

$$\epsilon_M = NuSc^{-1/3}\, Re^{-1/2} \left(\frac{X_b^*}{X_W^*}\right)^{1/3} \tag{21}$$

$$\epsilon_p' = \left(\frac{D_W^2}{\mu_W}\right)^{1/3} (\text{Property correction terms})^{-1/3} \tag{22}$$

Here departures in ϵ_M from unity represent the effect of physical property variations on the experimental data and

ϵ_p' represents the prediction of these effects from our analytical approximations. Instead of comparing the results with the predicted correction term ϵ_p', the variable properties were concentration averaged between the bulk and wall concentrations for each set of conditions. The correction term then becomes

$$\epsilon_p = \left(\frac{D^2_{AVE}}{\mu_{AVE}}\right)^{1/3} \tag{23}$$

The experimental and calculated values are recorded in Table 2. The values show increasingly good agreement as the difference between wall concentration and bulk concentration decreases. However, even at the totally polarized condition, the average property correction is within about 20% of the measured values. This is certainly adequate agreement for most design purposes and means extensive physical property data would not be necessary for good prediction of permeation rates.

Table 2. Experimental Evaluation of Approximate Models

$$\epsilon_M = NuSc^{-1/3}\,Re^{-1/2}\left(\frac{C_b^*}{C_W^*}\right)^{1/3}$$

Calculated from experimental data

$$\epsilon_p = \left(\frac{D^2_{AVE}}{\mu_{AVE}}\right)^{1/3}$$

Predicted from model

Bulk concentration gms/100 cc	ϵ_M	ϵ_p
	Total polarization	
1.47	0.42	0.35
7.8	0.55	0.42
	$\tau = 5.0$ psig.	
1.47	0.56	0.53
5.9	0.68	0.59
	$\tau = 1.5$ psig.	
2.2	0.66	0.68
5.9	0.73	0.73

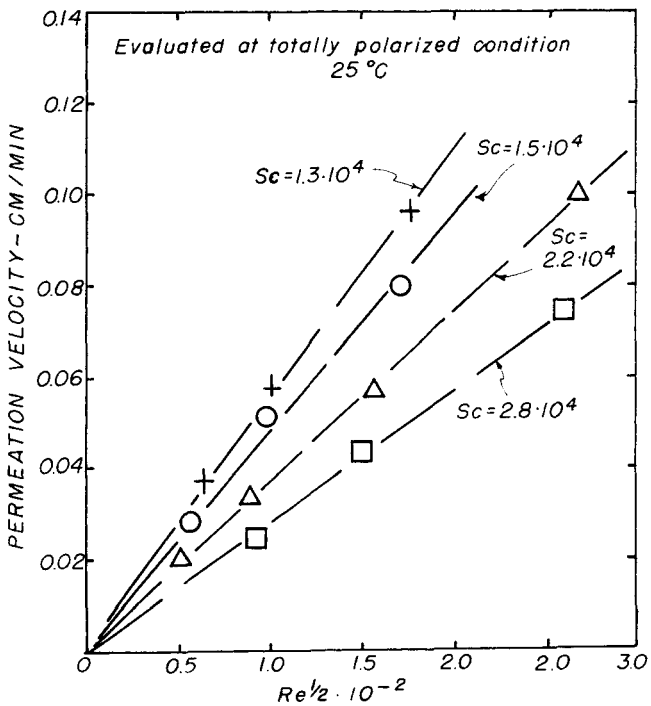

Fig. 5. Reynolds number correlation.

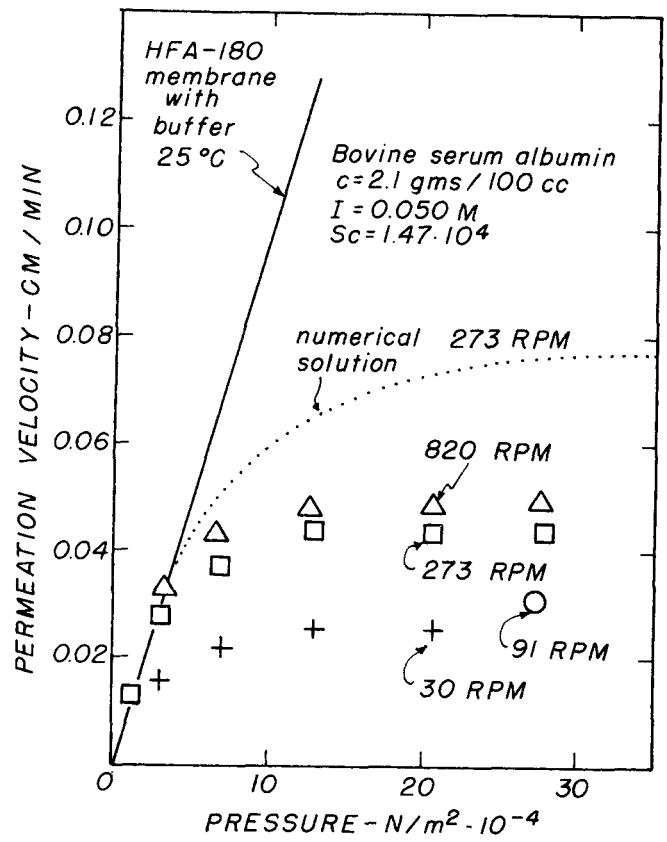

Fig. 6. Denatured protein permeation rates.

Effects of Protein Chemistry

The excellent prediction of the ultrafiltration of bovine serum albumin solutions is highly dependent on the hard sphere behavior of bovine serum albumin in high ionic strength solutions. Quite different results are shown in Figure 6 where conditions are similar to those of Figure 4 except that the ionic strength is lower by a factor of 5. Observed permeation rates are now about 50% less than predicted and significant hysteresis, not shown in this figure, was observed.

These effects appear to result from the instability of bovine serum albumin at low ionic strengths and in particular its tendency to undergo polymerization. The hysteresis effect suggests some degree of crosslinking and in fact when the membrane was checked after these runs, it was found to be covered by a mechanically stable film of protein. When tested, this film seemed to offer only negligible hydrodynamic resistance at low pressures but it appears likely that significant resistance is developed at more typical ultrafiltration pressures. Similar phenomena occur frequently in the much more complex systems of current industrial interest, but at present this behavior cannot be predicted in quantitative form.

Therefore, the predictions of boundary-layer theory appear to give only the maximum expected performance and that development of more reliable predictions will require an understanding of the denaturation behavior of the protein solutions processed.

EXTENSIONS TO OTHER GEOMETRIES

The above analysis although useful as a description of the protein boundary layer would not, in general, be expected to predict performance in the more complex geometries of practical importance. Of immediate interest would be to determine under what conditions our analytical approximation to rotating disk ultrafiltration could be used to predict common tube and parallel plate ultrafiltration. This reduces to finding a similarity solution to the two-dimensional duct flow problem which will simplify the analysis to a one-dimensional boundary layer. The flow about a rotating disk then can be included in this situation because although the analysis of it is based on the full three-dimensional Navier-Stokes equations, the resulting flow near the disk is consistent with the boundary layer hypothesis. The results of the rotating-disk analyses with the geometry dependent similarity transform could then be used to describe idealized transfer in these more refractory geometries.

Similarity Requirements

The diffusion equation for an arbitrary boundary layer duct flow and variable diffusivity can be written as follows using the usual boundary layer variables:

$$U_1 \frac{\partial X_p}{\partial X_1} + V_1 \frac{\partial X_p}{\partial Y_1} = \frac{\partial}{\partial Y_1} D \frac{\partial X_p}{\partial Y_1} \tag{24}$$

Density variations as discussed earlier are neglected as being second-order effects compared to diffusivity and viscosity variations for typical protein solutions. Diffusion transport in the x-direction has been neglected compared to convective transport. Even at creeping flow conditions, this should be a good assumption for protein solutions ($D \sim 10^{-8}$ cm^2/sec).

The boundary conditions presented for flow about a rotating disk apply here to the y-variations and additional restrictions are placed on the x-variations.

$$X_1 = 0 \qquad X_p = X_b \tag{25a}$$

$$Y_1 = 0 \qquad U_1 = 0 \tag{25b}$$

Inside the concentration boundary layer, the fluid dynamics may again be approximated by assuming constant shear stress across the boundary layer.

$$\mu' \frac{\partial U_1}{\partial Y_1} = \beta(X_1) \tag{26}$$

The external flow determines the geometry dependent shear stress distribution and also the pressure distribution.

The similarity transform developed by Acrivos (1960a) for variable property heat transfer can be extended to high mass transfer rates. To do this one seeks the conditions under which

$$X_p = X_1(\eta) \tag{27}$$

where

$$\eta = Y_1/\delta(X_1)$$

One can easily show by the transformation indicated by Equation (27) will be successful if

$$\delta(X) = Sc^{1/3} \beta^{-1/2} (3/2)^{1/3} \left[\int_0^X \beta^{1/2} dx_1 \right]^{1/3} \tag{28a}$$

$$\frac{V_0 \delta}{Sc} = \text{Constant} \equiv H_W \tag{28b}$$

Equation (24) then becomes

$$\frac{d}{d\eta} D \frac{d\theta}{d\eta} = -Sc \left(H_W + \int_0^\eta \int_0^\eta \frac{d\eta^2}{\mu} \right) \frac{d\theta}{d\eta} \tag{29}$$

with boundary conditions

$$\eta = 0 \qquad -Sc\,(\theta + 1)\, H = D \frac{d\theta}{d\eta} \tag{30a}$$

$$\eta = \infty \qquad \theta = 0 \tag{30b}$$

The results for the rotating disk can be directly transposed and used to predict the wall permeation rate if Equation (28b) is valid.

The general form of Equation (28b) is quite restrictive relative to the wide range of permeation rates which might occur in ultrafiltration. However, in situations where the velocity V is determined by the mass transfer process alone, Equation (11b), the total rejection boundary condition, would require precisely this form for V_W.

$$D \frac{d\theta}{d\eta}\bigg|_W = -H_W (\theta_W + 1) \tag{31a}$$

This is the usual situation which will allow a similarity transformation in diffusional boundary layers. Nevertheless, in ultrafiltration the permeation velocity is also determined by the imposed pressure.

$$-V_W = K (P_0 - P_{EXT} - \pi)$$

$$= K (\Delta P - \pi(\theta)) \tag{31b}$$

In general, P_0 is a different function of X than the mass transfer boundary layer thickness δ. This would invalidate, in general, the similarity transform for ultrafiltration.

It should be recognized at this point that a complete boundary layer prediction of the permeation behavior represented in Figure 4 is not necessary. If the high and low pressure asymptotes can be predicted, the intermediate region can be obtained by interpolation with a function having, for example, the following form:

$$V_W = \frac{K \Delta P}{1 + A \Delta P}$$

The low pressure asymptote is just the pure solvent resistance of the membrane and readily available. The high pressure asymptote is the critical permeation rate at total polarization which predicts maximum performance. This, then, is the region for which a prediction is needed.

At high degrees of polarization, the permeation rates shown in Figure 3 exhibit little if any response to pressure. This, also, has been observed as typical behavior in commercial type units (Fenton-May et al., 1971; Blatt et al., 1970) with solutions of large molecular weight materials. The behavior is actually very complex and the permeation rate is no longer determined by Equation (31b). The similarity transform is now possible because the velocity should be governed by the mass transfer process in this region. As discussed earlier, this solution will lead to an optimistic prediction of the best possible performance with factors such as sludging and gelling tending to lower the actual permeation velocity.

Actually the similarity result may be of wider application than this development indicates. Sparrow and Eckert (1962) have shown for the flat plate that for any reasonable distribution of V_W the local shear stress can be predicted to within 7% by using the similarity result. This lack of dependence of local values on upstream behavior would, of course, need to be tested for concentration polarization effects. Nevertheless, within the totally polar-

Table 3. Thin Channel Ultrafiltration
Predictions and Data

Protein conc., wt. %	Conditions** flow, cc/min.	Osmotic press, π $N/m^2 \cdot 10^{-4}$	Predicted flux cc/min. cm^2	Measured flux cc/min. cm^2
	1000	13.8	0.040	0.070
10	200	13.8	0.025	0.045
	200	total polar.	0.033	0.056*
	1000	13.8	0.060	0.11
1	1000	total polar.	0.080	0.12*
	200	13.8	0.036	0.09

Data from Blatt et al. (1970).
* The data were not taken at high pressures and the value represents an extrapolation.
** These data are subject to many qualifications:
1. Unit possibly not stabilized—values are optimistic.
2. Pressures are an average over channel length.
3. Temperature not reported, assumed room temperature—this would have a large effect on prediction.
4. Overall evaluation of data indicates an error of ~25-40% in measured fluxes.

ized region the similarity solution should be valid to within the ideal approximation that the proteins move only under concentration gradients.

The problem, except for the value of β, is mathematically identical to the rotating disk problem discussed earlier in this paper. The shear stress distribution can be determined from a description of the external flow. The value of β, the shear stress at the wall in a parallel plate duct at small flow rates, can be approximated by a constant equal to the value calculated for nonporous walls (Kozinski et al., 1970).

$$\beta \simeq Re^{-1/2}\,(L/U_R)\,(3Q_0/2Wb^2) \qquad (32)$$

This value can then be used to calculate the wall permeation rate given by Equation (b) in Table 1.

$$-V_W = Sc^{-2/3}\,Re^{-1/2}\left(\frac{X_W^*}{X_\infty^*}\right)^{1/3}\left(\frac{D_W^2}{\mu_W}\right)^{1/3}$$
$$(\text{corr. terms})^{1/3}\left(\frac{\beta}{X_1}\right)^{1/3} U_R$$

If, $U_R \equiv U_{AVE}$

$$Nu = -V_W L/D_{p\tilde{W}} = Sc^{1/3}\,Re^{1/3}\left(\frac{X_W^*}{X_\infty^*}\right)^{1/3}\left(\frac{D^2_{AVE}}{\mu_{AVE}}\right)^{1/3}\left(\frac{3L^2}{2bX}\right)^{1/3} \qquad (33)$$

This is the expected dependence on Reynolds and Schmidt numbers for laminar boundary layer mass transfer which can be tested for ultrafiltration with published data from thin channel units. The data of Blatt et al. (1970) were for bovine serum albumin in saline buffer using spiral 16 in. long ducts 1/4 in. wide by 0.01 in. high. The curvature of the duct is negligible compared to the boundary layer thickness, and thus the duct may be treated as a straight channel. Equation (33) was evaluated at average property conditions and at the average value of the function $(X^{-1/3})$. The results shown in Table 3 indicate that the predictions using these averages in Equation (33) are low but well within the accuracy of the data. This degree of accuracy is sufficient for many design estimates and indicates that the equation deserves further consideration. The expression is simpler and easier to apply to real situations than many current analyses.

ACKNOWLEDGMENT

This study was partially supported by a National Science Foundation grant. A. A. Kozinski was supported by a NSF traineeship throughout this study. The authors also thank the Amicon Corporation for information on their ultrafiltration units.

NOTATION

b = channel height
C_m = total molar concentration
D_{ij} = effective binary diffusion coefficient
$\mathcal{D}_{ij}$ = phenomenological transport coefficient
D = binary diffusion coefficient ratio D/D_b
d = disk diameter
F = dimensionless velocity function
g_i = total body force/unit mass of component i
H = dimensionless permeation velocity
K = permeation coefficient
L = characteristic length of channel
N_i = molar flux with respect to stationary coordinates
Nu = Nusselt number
P = pressure
Q_0 = volumetric flow rate
Re = Reynolds number
r = radial distance
Sc = Schmidt number
T = temperature
U_1 = boundary layer x direction velocity, $Sc^{1/3}\,U/U_R$
U_R = free stream reference velocity
V = permeation velocity
V_1 = boundary layer y direction velocity, $Sc^{2/3}\,Re^{1/2}\,V/U_R$
$\bar{v}$ = partial molar volume
W = width of channel
X_i = mole fraction
$(X_W^*/X_b^*) = \left(\frac{X_{pW}\,C_b}{X_{pb}\,C_W}\right)$
X_1 = boundary layer coordinate, x/L
Y_1 = boundary layer coordinate, $Sc^{1/3}\,Re^{1/2}\,y/L$

Greek Letters

β = shear rate at boundary
γ = activity coefficient
η = similarity coordinate transformation
θ = concentration ratio
μ_p = viscosity
μ = viscosity ratio $(\mu_p/\mu_p{}^0)$
$\tilde{\mu}$ = chemical potential
ν = kinematic viscosity
π = osmotic pressure
ρ_p = density of protein solution
ρ = molar density ratio
τ_{xy} = shear stress
Φ = volume fraction protein
$\tilde{\omega}$ = mass fraction
ω = disk speed

Subscripts

b = bulk conditions
ij = arbitrary species
0 = reference quantity
p = protein
s = solvent
W = wall
x, y = coordinate directions

LITERATURE CITED

Acrivos, A., "Solution of the Laminar Boundary Layer Energy Equation at High Prandtl Numbers," *Phys. Fluids*, **3**, 657 (1960).

———., "Mass Transfer in Laminar Boundary Layer Flows with Finite Interfacial Velocities," *AIChE J.*, **6**, 410 (1960).

Bird, R. B., et al., Transport Phenomena, Wiley, New York (1960).

Blatt, W. F., et al., "Solute Polarization and Cake Formation in Ultrafiltration: Causes, Consequences and Control Techniques," in Membrane Science and Technology, J. E. Flinn, (ed.), pp. 47-97, Plenum Press, New York-London (1970).

Cochran, W. G., "The Flow Due to a Rotating Disk," *Proc. Camb. Phil. Soc.*, **30**, 635 (1934).

Emanuel, A. S. and D. R. Olander, "High Flux Solid-Liquid Mass Transfer," *Intern. J. Heat Mass Transfer*, **5**, 539 (1964).

Fenton-May, R. I., et al., "The Use of Pressure Driven Membrane Processes in the Dairy Industry," *Membrane Separations Symp.*, 68th Ann. Am. Inst. Chem. Engrs., Houston (1971).

Ford, T. F., "Viscosity-Concentration and Fluidity-Concentration Relationships for Suspensions of Spherical Particles in Newtonian Liquids," *J. Phys. Chem.*, **64**, 1168 (1960).

Keller, K. H., et al., "Tracer and Mutual Diffusion Coefficients of Proteins," *J. Phys. Chem.*, **75**, 379 (1971).

Kozinski, A. A., and E. N. Lightfoot, "Ultrafiltration of Proteins in Stagnation Flow," *AIChE J.*, **17**, 81 (1971).

Kozinski, A. A., "Ultrafiltration of Protein Solutions," Ph.D. thesis, University of Wisconsin, Madison (1971).

———., et al., "Velocity Profiles in Porous-Walled Ducts," *Ind. Eng. Chem. Fundamentals*, **9**, 502 (1970).

Olander, D. R., "The Influence of Physical Property Variations on Liquid-Phase Mass Transfer for Various Laminar Flows," *Intern. J. Heat Mass Transfer*, **5**, 765 (1962).

Oncley, J. C., eet al., "Physical-Chemical Characteristics of Certain of the Proteins of Normal Human Plasma," *J. Phys. Chem.*, **51**, 184 (1947).

Scatchard, G., et al., "The Osmotic Pressure of Plasma and of Serum Albumin," *J. Clinic. Invest.*, **23**, 458 (1944).

Scattergood, E. M., and E. N. Lightfoot, "Diffusional Interactions in an Ion Exchange Membrane," *Trans. Farad. Soc.*, **64**, 1135 (1968).

Sparrow, E. M., and E. R. G. Eckert, "Sensitivity of Skin Friction and Drag to the Distribution of Suction or Blowing," *J. Aero/Space Sci.*, **29**, 104 (1962).

Stewart, W. E., "Forced Convection in Three-Dimensional Flows: I. Asymptotic Solutions for Fixed Interfaces," *AIChE J.*, **9**, 528 (1963).

Tanford, C., Physical Chemistry of Macromolecules, Wiley, New York (1961).

Wagner, M. L., and H. A. Scheraga, "Gouy Diffusion Studies of Bovine Serum Albumin," *J. Phys. Chem.*, **60**, 1066 (1956).

APPENDIX A. EXPERIMENTAL SYSTEM CALIBRATION

Although the experimental system shown in Figures 1 and 2 appeared to meet all design requirements, its performance was also checked experimentally by measuring the rate of dissolution of a benzoic acid disk occupying the place of the membrane and its support. This is a standard technique in mass transfer investigations and is convenient because the low solubility of benzoic acid permits one to neglect both variations in transport properties and interfacial velocities. The theoretical transfer rate can then be analytically calculated from the known velocity profile Cochran (1934). The following solution is obtained:

$$Nu = 0.60 Sc^{1/3} Re^{1/2}$$

Excellent agreement between experiment and theory have been shown by other investigators (Emanuel and Olander, 1964) using benzoic acid, and thus the mass transfer measurements should be a good test of our system design.

Experimental transfer rates, measured spectrophotometrically, are compared with the prediction in Figure A1. The low

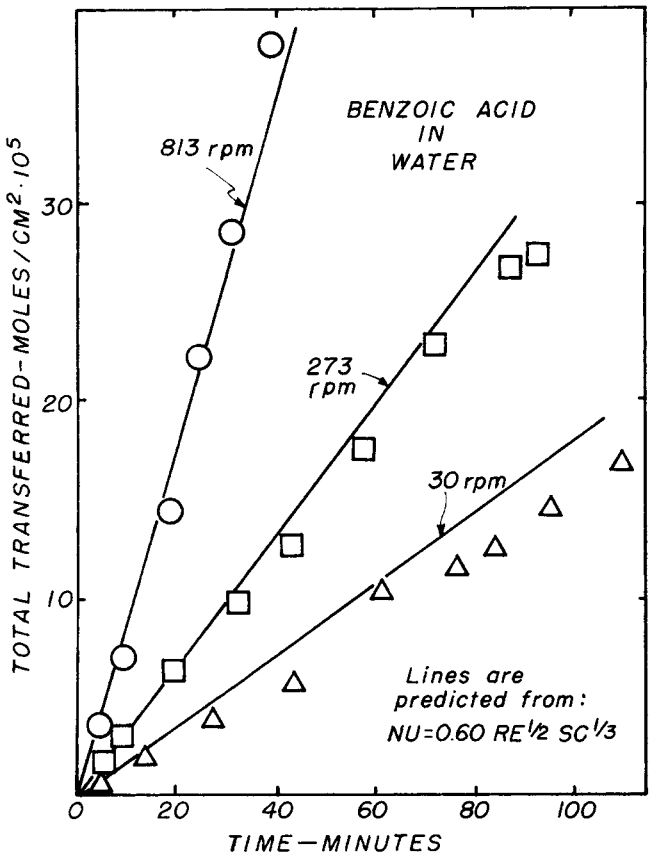

Fig. A1. Benzoic acid calibration.

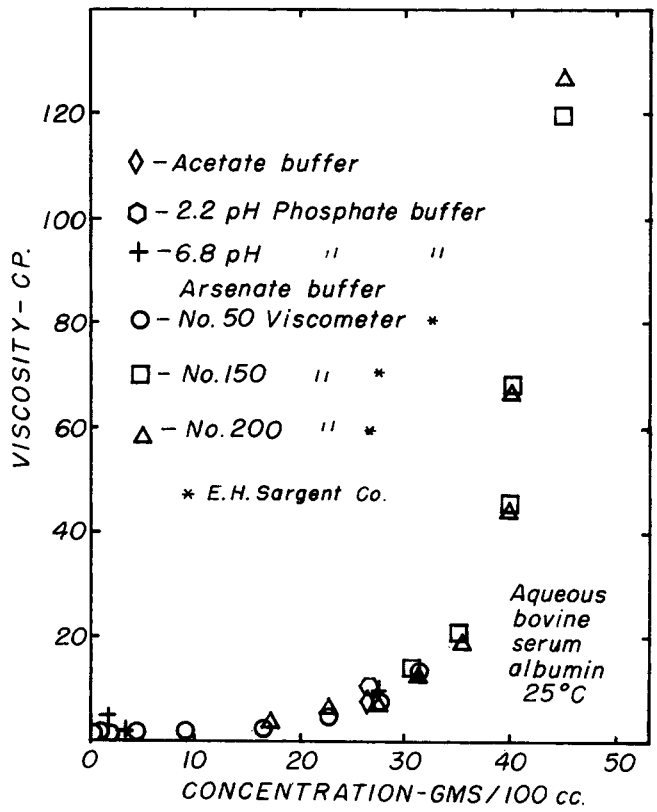

Fig. A2. Viscosity-bovine serum albumin solutions.

TABLE B1. VISCOSITY CONCENTRATION MODELS

Model form	Variance of prediction	Constants	99% Confidence limits	Comments
$\frac{1}{\mu_p} = \alpha + \beta c + \gamma c^2$	0.00027	$\alpha = 1.11$ $\beta = -0.0542$ $\gamma = 6.71 \cdot 10^{-4}$	± 0.019 ± 0.0022 $\pm 0.5 \cdot 10^{-4}$	Preferred model has discontinuity where μ is infinite.
$\frac{1}{\mu_p} = \alpha + \beta c + \gamma c^2 + \xi c^3$	0.00017	$\alpha = 1.12$ $\beta = -0.0607$ $\gamma = 0.00106$ $\xi = -5.78 \cdot 10^{-6}$	± 0.016 ± 0.0046 ± 0.00026 $\pm 3.6 \cdot 10^{-6}$	Addition of C^3 term does not significantly improve fit, but residuals are more satisfactory.
$\mu_p = \exp(\alpha c^2)$	0.0056	$\alpha = 0.00244$	$\pm 0.56 \cdot 10^{-4}$	μ asymptotically approaches infinity.

experimental values at low disk speeds are probably due to poor mixing. Also, edge effects are large at low disk speeds. In general, the excellent agreement between theory and experimental data indicates that the hydrodynamic model of an infinite disk rotating in an infinite volume of quiescent fluid is realized in our system.

APPENDIX B. PHYSICAL PROPERTIES

Rheology of Serum Albumin

Globular protein solutions have generally been considered Newtonian over their entire concentration range. This belief is based on the rigid, nearly spherical shape (axis ratio < 3 to 1) of globular proteins particularly near their isoelectric point. However, this author was unable to find an experimental confirmation of Newtonian behavior for serum albumin in concentrated solutions, and thus an experimental check was desirable.

The viscosity of serum albumin solutions at 25°C over a wide range of concentrations were obtained in this study using Ostwald viscometers. Three different sizes of viscometers were used so that the presence of non-Newtonian effects over the shear range of the study could be determined. All other conditions being the same, average shear rates should vary by at least a factor of 5 between viscometers. The viscometers used in this study were also chosen so that kinetic effects would be negligible. All viscometers were calibrated with glycerol-water mixtures at 25°C over a range of viscosities.

The majority of the viscosity measurements were made in arsenate buffer—0.5 M ionic strength 6.7 pH. The arsenate buffer is easier to use over a long period of time because it prevents growth of microorganisms which ordinarily occurs with phosphate buffers exposed to air. Several check measurements were made with phosphate buffers at different ionic strengths and pH and no significant effects were found. A check with 0.1 M acetate buffer was also made because the available literature values for serum albumin diffusivities were with acetate buffer. The values again were not different significantly from the values with arsenate buffer.

Non-Newtonian Effects

The measured viscosities of serum albumin shown in Figure B1 did not indicate any significant differences due to viscometer diameter. This confirms the expected Newtonian behavior up to a protein concentration of 45 g/100 cc for these shear rates. Beyond this point accurate measurements could not be made with the Ostwald viscometers due to the extremely high viscosities of these concentrated solutions. The solubility limit was measured to be about 58.5 g/100 cc. At this limit the protein solution was nearly an immobile gel.

Published viscosity data (Oncley, 1947; Tanford, 1961), which is available only at low concentrations, is in excellent agreement with our measured values. Our data show an intrinsic viscosity $[\eta]$ of 3.75 cc/g as compared to the value of 3.7 cc/g reported by Tanford (1961).

The concentration dependence of the viscosity was statistically fitted and a summary of the satisfactory models is given in Table B1. The reciprocal second-order power-law model was selected for use in later analyses both because of simplicity and resemblance to the Einstein equation. However, the other two models were equally good empirical representations of the data.

Diffusion Coefficients

Serum albumin is one of the few proteins for which extensive diffusion data are available. Wegner and Scheraga (1956) have determined that the diffusivity of serum albumin has a linear concentration dependence over the concentration range 0.25 to 1.25 g/100 cc. More complete data have been recently obtained by Keller et al. (1971) over the concentration range of 1.0 to 32 g/100 cc. These data were used in our developments in the following form:

$$\frac{D_{pW}}{D^0_{pW}} = 0.13 + 0.87 \exp(-1.2\,\Phi)$$

$$D^0_{pW} = 7.1 \cdot 10^{-7}\ \text{cm}^2/\text{sec at } 25°\text{C}$$

This functional form, while different from that presented by Keller et al., seemed to fit their data equally well. As was true of our viscosity measurements, several other functions could also be empirically fit to their data. The discrimination between forms would occur at extremely high concentrations where data at present are not available.

Osmotic Pressure Data

Scatchard et al. (1944) has derived a rigorous expression for dilute solutions which accounts for all factors influencing the osmotic pressure such as ionic strength pH and excluded volume. He and his co-workers have made a complete experimental study of these effects with serum albumin. With dilute solutions (< 5 g/100 cc) the osmotic pressure is a strong function of the charge on the protein (pH dependence). At 6.8 pH, the following expression was developed from their measurements.

$$P = 448.2\ \omega_p\ (1 + 0.087\ \omega_p) \qquad P - N/m^2$$
$$\omega_p = \text{g protein/100 g water}$$

Additional data were also taken by Scatchard et al. up to a protein concentration of 30 g /100 cc. The authors did not report a functional form for the high concentration data. A replot of their data between 5 and 30 g/100 cc indicated that a parabolic equation was an excellent representative of all of their data between 3 and 30 g/100 cc.

$$P_\pi = 89.63\ C_p^2 \qquad P_\pi - N/m^2$$

This expression is valid at 25°C, 7.4 pH, and 0.15 M NaCl. However, at high concentrations, the data did not indicate a significant effect of pH so that the expression should be valid at 6.8 pH. The equation would be useful in converting membrane pressure drops to interfacial concentrations.

Manuscript received January 20, 1972; revision received June 2, 1972; paper accepted June 2, 1972.